Compact Doppler magnetograph

A. Ruzmaikin[1], P. I. Moynihan, A. H. Vaughan

Jet Propulsion Laboratory,
Pasadena, CA 91109, USA

A. Cacciani

University of La Sapienza, Rome, Italy

ABSTRACT

The Compact Doppler magnetograph is designed to be a low-cost flight instrument that images the full solar disk through two narrowband filters at the red and blue "wings" of the solar potassium absorption line. The images are produced on a 1024x1024 charge-coupled device with a resolution of 2 arcseconds per pixel. Four filtergrams taken in a very short time at both wings in the left and right states of circular polarization are used to yield a Dopplergram and a magnetogram simultaneously. The noise-equivalent velocity associated with each pixel is less than 3 m/s. The measured signal is linearly proportional to the velocity in the range ± 4000 m/s. The range of magnetic fields is from 3 to 3000 Gauss. The optical system of the instrument is simple and easily aligned. With a pixel size of 12 μm, the effective focal length is 126 cm. A Raleigh resolution limit of 4 arcseconds is achieved with a 5-cm entrance aperture, providing an *f*/25 focal ratio. The foreoptic is a two-component telephoto lens serving to limit the overall optical length to 89 cm or less. The mass of the instrument is only 14 kg. The power required is less than 30 Watts. The Compact Doppler Magnetograph can be used in space missions with severe mass and power requirements. It can also be effectively used for ground-based observations: Large telescope, dome or other observatory facilities are not required

Keywords: Doppler, magnetic field, spacecraft imaging, solar instrumentation

1. INTRODUCTION

One of the most important elements of the NASA Sun-Earth Connection Program is the solar magnetic field: its generation inside the Sun (dynamo), its appearance on the solar surface, and its influence on the corona and solar wind. Recently, helioseismology permitting the study of the solar interior has been developed[1]. The basic observational tools of helioseismology are Dopplergrams and magnetograms carrying information on velocity and magnetic fields on the solar surface.

The resolution of ground-based instruments designed to observe the solar magnetic and velocity fields is limited by atmospheric "seeing," and, in many cases, by weather conditions. In addition, most high-performance ground instruments use spectroscopic methods that make them very expensive (the typical cost exceeds $0.5 million). Essential cost savings can be achieved with the use of filter-type instruments. The only space instrument of this type, successfully working onboard the SOHO spacecraft, is the Michelson Doppler Imager designed at Stanford and Lockheed[1]. This instrument has a 12.5 cm telescope aperture, an effective focal length of 186.7 cm, and a 4-arcsecond full-disk resolution (plus a 1.2-arcsecond resolution to observe small regions near the center of the Sun). Its noise performance is 20 m/s for the velocity and 20 Gauss for the magnetic field. The mass of the instrument is 58.5 kg.

Here we present a design for a high-performance, compact, low-cost flight instrument that measures velocity and magnetic fields on the photosphere. This instrument is called the "Compact Doppler Magnetograph", or CDM, and is based on the magneto-optical filter invented by A. Cacciani. Ground instruments based on this filter are currently operating in Hawaii, Treffen in Austria, and Mount Wilson, Big Bear, and Mojave Solar in Southern California. The design uses heritage from a JPL instrument proposed for SOHO[2]. The current design includes technical refinements that improve performance, extend lifetime, make it light and compact, and reduce the cost.

---

[1] Send correspondence to A. Ruzmaikin, E-mail: aruzmaik@pop.jpl.nasa.gov

2. INSTRUMENT DESCRIPTION

The Compact Doppler Magnetograph is an imaging instrument that simultaneously produces Dopplergrams (images of a velocity field) and magnetograms (images of a magnetic field). The instrument images the full solar disk at the wavelength of the potassium D2 line (769.9 nm) or the sodium D1 line (589.6 nm). These photospheric lines are stable and narrow, enabling high sensitivity for magnetic and velocity fields.

2.1. The magneto-optical filter

The heart of the instrument is a highly stable magneto-optical filter (MOF) that selects narrow bands at the red and blue wings of the solar absorption line (see Figure 1).

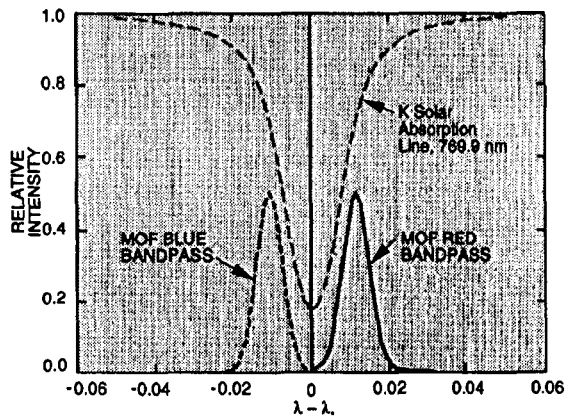

Figure 1. Two narrow (0.02 nm) bands are selected at the blue and red wings of the solar potassium absorption line.

The working principles of the filter, described in [3-5], are illustrated in Figure 2. The filter is a glass cell that maintains a potassium (or sodium) vapor in a longitudinal magnetic field (about 2 kGauss). Without the magnetic field, two crossed linear polarizers stop the light transmission through the cell. With the magnetic field, the transmission in two narrow wavelength bands around the absorption resonance line of the vapor becomes possible due to the Faraday rotation in the wings of the spectral line and due to the Zeeman effect. To understand the last effect one has to present the linearly polarised light entering the cell as the sum of left- and right-handed circular polarizations. An atom excited to a Zeeman level can absorb only one of the polarizations, transmitting the other. Due to the difference in energy levels, hence absorbtion coefficients for the two polarizations, the light will be left polarized in one wavelength band and right polarized in the other wavelength band. Being presented now as a sum of two linear polarizations, the light passes the second polarizer.

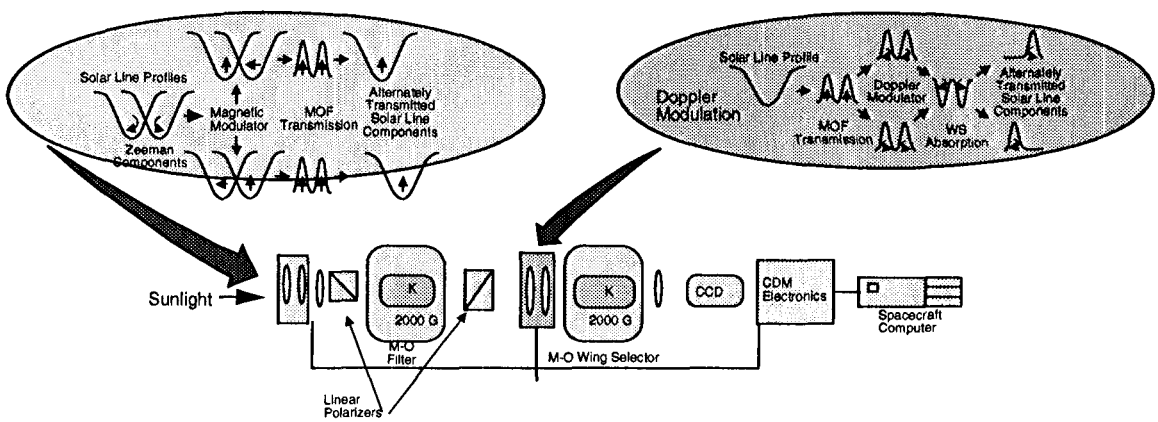

Figure 2. Two absorption cells and two modulators are used in the Cacciani filter to absorb a solar line and select its blue and red narrow bands in both circular polarizations.

The two bands are then separated by the second filter, which is called the wing selector (see Figure 2). The wing selector requires a quarter-wave retardation plate in front of the cell at 45 degrees with respect to the second polarizer to convert the linear polarization into circular polarization. This allows the wing selector to absorb only one of the bands passed through the first cell, again due to the Zeeman effect. The selection of another band is achieved with the help of an electro-optical modulator that alternates the retardation axis ± 45 degrees. A magnetic modulator in front of the first cell allows selection of different polarizations of the solar absorption line. For each band (red or blue) two images are taken, one for each state of polarization, i.e., four in total. From these four images, one Doppler and one magnetic image are created, as illustrated in Figure 3. Thus, Dopplergrams and magnetograms are determined simultaneously. About 20 such determinations are sufficient to achieve an accuracy of 3 m/s in velocity and 3 Gauss in magnetic field at a signal-to-noise ratio of unity. Simultaneous image acquisition helps to discriminate between true signals and spurious signals due to crosstalk[3]. The signal is proportional to the velocity in the range ±4 kilometers per second.

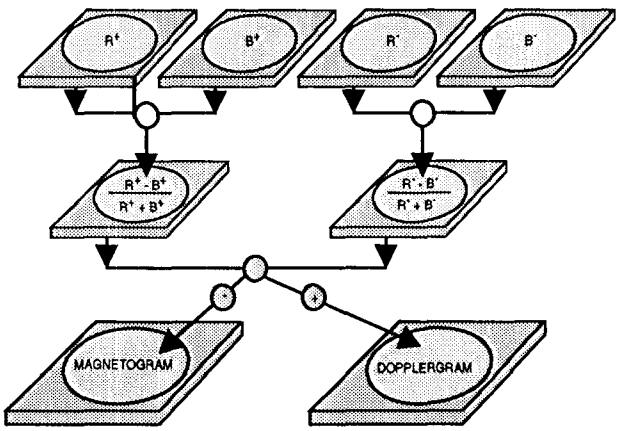

Figure 3. A Dopplergram and a magnetogram are formed from four filtergrams taken at red (R) and blue (B) wings of the absorption line in two circular polarizations ± .

The use of potassium, advanced glass, and simple vapor deposition control assures that the cell's lifetime will exceed a typical mission lifetime of several years. The lifetime of earlier MOFs had been limited by cracking caused by metallic vapor attacking the surface of the glass. Early MOFs, using sodium in quartz, had a short lifetime. The use of the potassium vapor, which is much less active, and which evaporates at a temperature 100°C lower than the sodium one, prolongs the lifetime. Glass resistant to potassium vapor must be used. The vapor deposition on the glass is controled by external heating coil. Potassium MOFs in an instrument in Hawaii have been working successfully for more than three years [Tomczyk, private communication]. It is more difficult but possible to fabricate long-living sodium cells now[5].

2.2. Mechanical configuration

The magneto-optical filter, wing selector, and required optics are containedin a thermally controlled, partially pressurized enclosure. The CCD imager and the instrument electronics are attached to one end (see Figure 4).

Optics Cover: The optics cover is opened after launch by a spring-loaded, rotating shaft actuator held in place by a restraining pin and is commanded open by the microcontroller. This mechanism has been successfully used on space missions.

CCD Imager: The baseline imager for the CDM utilizes a spare 1024x1024 CCD detector (from the Cassini mission to Saturn) with nominal 12-μm pixels and a 12-bit analog-to-digital converter. An exposure time, or integration time of 0.125 seconds, is dictated by the CCD readout rate, based upon reading four Megapixels per second with a two-signal-chain device. This exposure time necessitates a mechanical shutter to eliminate pixel smear. A rotating shutter of the flight design produced by Lockheed is proposed as it readily delivers the required exposures with minimal power consumption (less than 10 Watts). The images are then read into a field-programmable gate array buffer where pixel registration is accomplished, after which the "red" and "blue" images are subtracted, the result is added to the previous image sum, and the new sum is restored. The buffer has a 32-Megabit storage memory. Eight images per second can be produced, resulting in the summation of 480 images per minute, 240 each for the Dopplergrams and magnetograms. This provides a comfortable margin over the minimum required to produce a 3 m/s velocity accuracy. At the end of each minute, the final image is transferred to the spacecraft computer for storage and final signal compression prior to transmission to the NASA Deep Space Network on

Earth. An image will also be transferred from the CCD buffer to the spacecraft computer to facilitate spacecraft attitude control. The baseline imager configuration is a modification of the JPL design flown on the Air Force MILSTAR satellite in 1995. The required design change for the CDM is a straightforward adaptation of the new CCD into a 12-bit format. The electronics and shutter are integrated into the aft end of the CDM, with the CCD mounted at the optical focal plane. All critical electronic parts are radiation-hardened. A thermoelectric cooler maintains the CCD temperature of 10°C (± 0.1°C) , sufficient to eliminate sensitivity variations due to temperature.

APS (active pixel sensor) Imager: An APS imager could be used in place of a CCD, especially for cases severely constrained in mass and power. The APS detector is a CMOS-compatible technology recently developed at JPL[6]. The APS features the same sensitivity and performance as the CCD but with many additional improvements. In the APS, active transistors are located within each pixel to amplify and buffer the signal. Because of the individual addressibility of each pixel, the APS has random access capability. It also has easy window-of-interest readout, nondestructive readout for signal-to-noise improvement, simplified clock voltages, and easy integration with other on-chip signal elements. The timing, control, and signal-chain electronics are designed to be integral with the chip, along with the detector, rendering a "thumbnail" size for the total assembly. As a result, only a single +5-Volt source is required for APS operation.

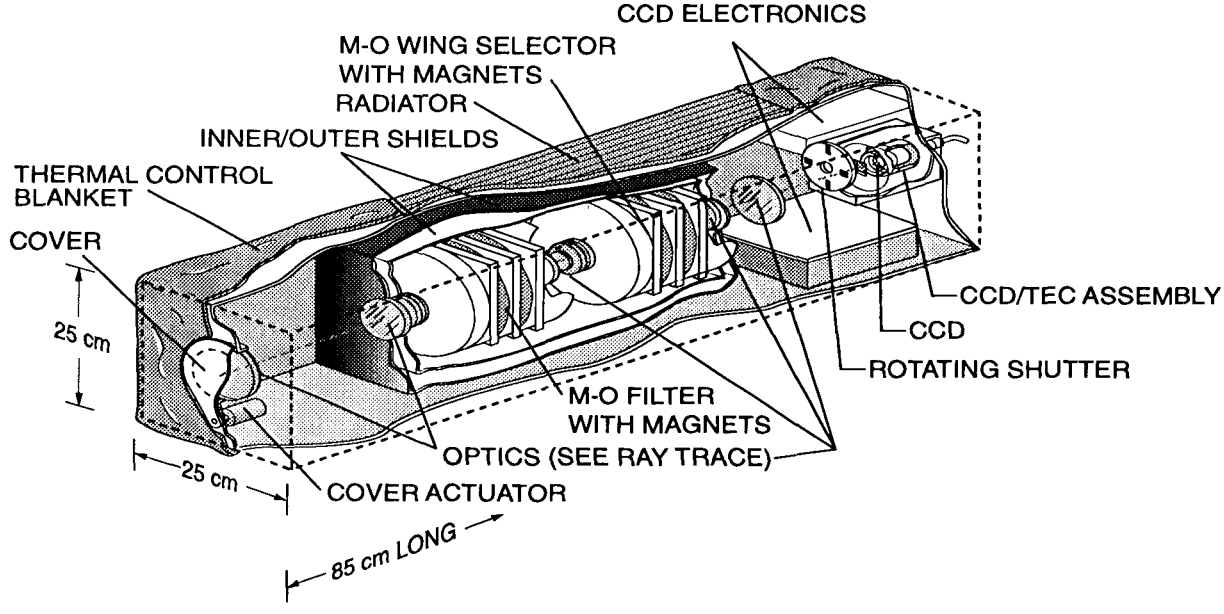

Figure 4. Mechanical assembly of flight instrument.

2.3. Optical system

The optical system is simple and easily aligned (see Figure 5). With an image scale of 2 arcseconds per pixel, the effective focal length (EFL) is 126 cm. A Raleigh resolution limit of 4 arcseconds is achieved with a 5 cm entrance aperture, providing an *f*/25 focal ratio. The foreoptic is a two-component telephoto lens serving to limit the overall optical length to 89 cm or less. A ~1:1 relay produces an intermediate pupil and a second focal plane yielding the required magneto-optical filter beam diameter and system EFL. The relay contains a field lens at the first focal plane, followed by a two-element reimaging lens near the pupil image. The beam diameter does not exceed 1 cm over the path length of up to 35 cm occupied by the magneto-optical filter and wing selector. Diffraction-limited performance is achieved with mildly aspheric lenses.

To avoid pixel saturation at 125 milliseconds exposure time (with full-well capacity $\approx 10^5$ electrons), a reflective attenuating filter having nominally about 2-percent transmittance is used as the first element of the system. This filter also substantially reduces the heat load on the instrument.

The optical system can be simplified by eliminating the relay and placing the magneto-optical filter and beam selector directly in the converging beam from the foreoptic, at the expense of increased beam size (becoming approximately 1.7 cm) in

the magneto-optical filter. Since the smaller beam size is desirable to minimize further the effects of any nonuniformities in the magneto-optical filter, the relay in the current design has been retained, but possible simplification could be considered as an option. Although the system will operate practically monochromatically at 770 nm, prelaunch alignment will be simplified by making the optical system achromatic so as to be confocal at both 770 nm and the HeNe laser wavelength of 633 nm.

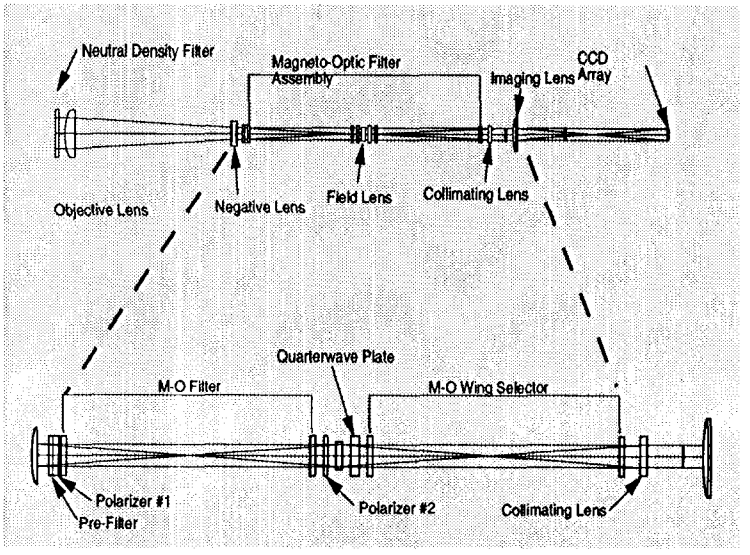

Figure 5. Coaxial optical system offers simplicity and compactness.

3. SPACECRAFT CONNECTION

3.1. Pointing system

In the present design, all course and fine guidance required by the instrument must be provided by the spacecraft. Modern spacecraft are capable of a pointing stability of 1 arcsecond per second. To minimize spacecraft jitter and drift during the imaging sequence, dynamic image registration can be used to correlate adjacent images. This method will provide 0.1-pixel interimage correlation for critical observations. In case the spacecraft can provide only coarse guidance, a fine-guidance gimbal system attached to the instrument can be built. However, this will increase the mass and cost of the instrument. (Gimbal systems are not discussed here.)

3.2. Command and control

The operation of the CDM instrument is governed by a microcontroller command and control system that controls the shutter, CCD image buffer, temperature control electronics, magneto-optical filter polarization functions, and optics cover actuator. The microcontroller also serves as the primary command interface between the instrument and the spacecraft. The logic components of this system are high-speed, radiation-hardened, latchup-resistant CMOS large-scale and very large-scale integrated circuits. These components reduce the mass, power consumption, and overall electronics part count. The major components are a dedicated microprocessor, an interrupt controller, a timing control unit, and a memory subassembly.

3.3. Power supply

Power for the instrument is received from the spacecraft bus via a current-limited load switch. The power supply converts the received 28 Volts (±4 Volts) bus power to the multiple output voltages required of the CDM. Voltage regulation and ripple are held to ±0.1 Volt. The imager electronics, the magneto-optical filter, and the thermal control are the major load groups.

3.4. Thermal control

The instrument is conductively and radiatively isolated from the spacecraft and maintained within a temperature range of 0-40°C. The two heater elements (1 cm x 0.5 cm) for each potassium cell within the magneto-optical filter operate at a nominal temperature of 150°C. Heat is removed directly to space through a radiator mounted on the outboard side of the instrument sensor assembly enclosure. The radiator surface is designed to have a low solar absorptivity (0.2) and high-infrared emissivity (0.8) so that short-term direct solar input can be accommodated (up to 30 minutes of operation). The 0.112-square-meter radiator is sufficient to reject 30 Watts operating at 20°C with a 20-percent field-of-view blockage.

3.5. Possible space applications

The instrument is well suited for solar missions limited by weight and cost. Two examples are pointed out below: The Compact Doppler Magnetograph has been included in a NASA SMEX proposal (JPL Project "MagSonas"). The low-cost design proposed was an instrument with a mass of 14 kilograms, a size of 85x15x15 cubic cm, power of 30 Watts, and noise level of 3 m/s in velocity and of 3 Gauss in magnetic field. A possible application is the future NASA Solar Stereo Mission. For this mission, the CDM mass can be reduced to less than 10 kilograms and vector measurements can be made. The essential cost reduction is possible as well.

4. GROUND-BASED INSTRUMENTATION

As mentioned in the Introduction, there are several ground-based instruments effectively operating at a number of US and European observatories. A new ground-based instrument using similar technology has been designed by the EDDY Company in Apple Valley, California. The presently operating version of the instrument has a small aperture (about 1 centimeter) so that the resolution of the images is low (8 arcseconds). The simultaneous Dopplergrams and magnetograms are taken at standard video rate (one-thirtieth of a second), allowing a very good signal-to-noise ratio. A collaborative effort between JPL and the EDDY Company is being considered for hardware development and the use of the Mojave Solar Observatory as a test site for flight instruments.

APPENDIX

Imaging parameters

The following basic parameters and constraints are assumed for the Compact Doppler magnetograph:

Table 1.

λ_0 = 769.9 nm potassium (λ_0 = 589.6 nm sodium)	Central wavelength
p = 12 μm	CCD pixel pitch for TI 1024 array
L = 1.0 AU	Distance of spacecraft from Sun
N_{Sun} = 980	Required no. of pixels across solar diameter
N_{Airy} = 4	Required no. of pixels across Airy disk
R_{Sun} = 960 arcsec	Solar radius at 1 AU

The parameters in Table 1 imply the imaging and photometric parameters presented in Table 2.

Table 2.

EFL = 126.4 cm	Effective focal length
Scale = 2 R_{Sun} /N_{pixels}=1.958 arcsec/pixel	Image scale
D = 4.95 cm	Diffraction-limited telescope aperture diameter
F = 25.6	Telescope *f*/number
A_p = 1.44	Pixel area
A_T= 19.2 cm^2	Telescope collecting area
$\Omega^+ = 9.02x\ 10^{-11}$ sr	IFOV per pixel, steradians
$A_T^+ = 1.77x\ 10^{-9}\ cm^2$ sr	System A+ product (Lagrange invariant)

In addition we assume the efficiency factors that are given in Table 3.

Table 3.

QE = 0.6	Detector quantum efficiency
τ_{lens} = 0.96	Lens transmittance
τ_{pre} = 0.6	Prefilter peak transmittance
τ_{ND} = 0.02	Neutral density filter transmittance

The resultant system transmittance is $\tau_{sys} = \tau_{lens}\ \tau_{pre}\ \tau_{ND} = 0.0115$. The ND filter is used in order to increase the CCD exposure time to a value compatible with the maximum allowable CCD readout rate. The ND filter will be located in front of the first optical element of the imager, where its effect also will be to reduce the heat load into the instrument.

Absorption line

For purposes of computation it is convenient to represent the solar potassium absorption line by a synthetic intensity profile given by

$$T_{phot}(\lambda) = e^{-\alpha(\lambda)}$$

where the atomic absorption coefficient with damping and Doppler broadening is taken to be

$$\alpha(\lambda) = \alpha_0 \frac{a}{\pi} \int_{-10}^{10} \frac{e^{-x^2} dx}{a^2 + [u(\lambda) - x]^2}$$

Here a is the damping parameter and

$$u(\lambda) = \frac{\lambda_0 - \lambda}{\lambda} \frac{c}{V_0}$$

where V_0 is the most probable atomic velocity. For potassium (atomic mass M = 39.103x1.66x10^{-24} g), $V_0 = (2kT/M)^{1/2}$ = 1.57 km/s. By suitably adjusting a and V_0 we obtain a reasonably good fit to an observed potassium line profile. The "best fit" empirical values a = 0.9 and V_0= 1.8 km/s are adopted here.

Magneto-optic filter passbands

For purposes of estimation we represent the two passbands (red and blue) of the magneto-optic filter by Gaussian profiles of the form

$$\tau_{RED}(\lambda) = \tau_{MOF} \exp\left[-(\frac{\lambda - \lambda_{R0}}{FWHP})^2\right]$$

and

$$\tau_{BLUE}(\lambda) = \tau_{MOF} \exp\left[-(\frac{\lambda - \lambda_{B0}}{FWHP})^2\right]$$

where $\lambda_{R0} = \lambda_0 + \Delta\lambda_{Zeeman}$, $\lambda_{B0} = \lambda_0 - \Delta\lambda_{Zeeman}$ are the central wavelengths of the passbands, separated from λ_0 by the Zeeman shift

$$\Delta\lambda_{Zeeman} = \lambda_0^2 \, B \, g \, 4.668x10^{-5} \text{ cm.}$$

For magnetic field strength B=3000 Gauss and Lande factor g=1.54 the resulting shift (adopted here) is $\Delta\lambda_{Zeeman}$ = 0.012 nm.

We further adopt arbitrarily the value 0.5 for the peak transmittance of MOF and used FWHP=0.004 nm, yielding approximate MOF profiles in fair agreement with measured values. Since this crude model ignores polarization, it is useful only for the purpose of estimating the difference signals to be expected from line-of-sight velocity changes (Doppler shifts). The resulting approximate solar potassium absorption line profile and MOF passbands are illustrated in Fig. A1, for an assumed solar line-of-sight velocity offset of 2000 m/s relative to the rest frame of the MOF (i.e., the spacecraft).

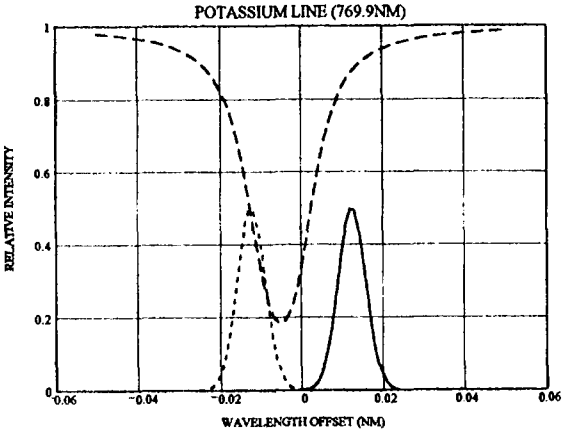

Figure A1. Synthetic solar photospheric absorption line profile and MOF passbands. The solar line is shown for a line-of-sight velocity offset of 2 km/s.

Magneto-optic filter signal

The MOF signals (the measured numbers of electrons) in the red and blue passbands are given, for an integrating time Δt, by the integrals

$$RED = \Delta t \tau_{sys} \tau_{MOF} A_T \Omega_p QE \int_{\lambda_0 - 0.1nm}^{\lambda_0 + 0.1nm} I_{phot}(x - \Delta\lambda) \tau_{RED}(x) N(x,T) dx,$$

$$BLUE = \Delta t \tau_{sys} \tau_{MOF} A_T \Omega_p QE \int_{\lambda_0 - 0.1nm}^{\lambda_0 + 0.1nm} I_{phot}(x - \Delta\lambda) \tau_{BLUE}(x) N(x,T) dx$$

where $\lambda_D = \Delta\lambda$ v/c is the Doppler shift of the solar line for line-of-sight velocity v and N (λ,T) is the Planck function approximating the photospheric continuum (T = 5800 K). For the parameters adopted, these integrals yield values close to the likely full well capacity of the CCD (100,000 electrons), when the integrating time is taken to be the smallest allowed value (125 ms).

It is convenient to define a "Doppler Parameter"

$$Q = \frac{BLUE - RED}{BLUE + RED}.$$

The signal-to-noise ratio for a single exposure is evidently

$$SNR = \frac{BLUE - RED}{\sqrt{BLUE + RED + Nr^2}}$$

where Nr ≈ 55 e^- is the read noise. Let SNR_N be the signal-to-noise ratio to be achieved by adding N single exposures:

$$N = \left(\frac{SNR_N}{SNR_1}\right)^2.$$

The Doppler Parameter Q computed from the foregoing is plotted as a function of line-of-sight velocity in Fig. A2.

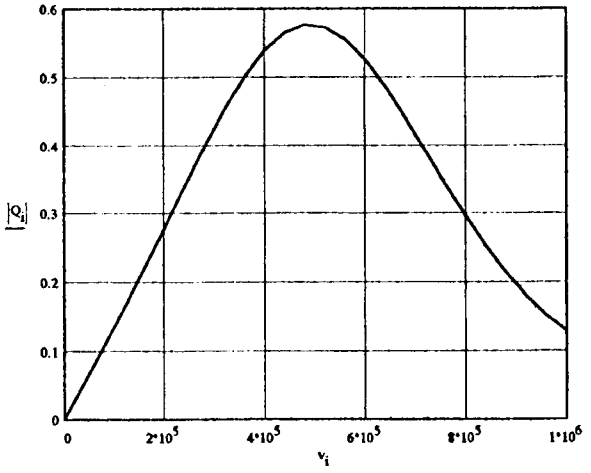

Figure A2. MOF Doppler signal Q as a function of line-of-sight spacecraft speed in cm/s.

It can be seen that Q increases nearly linearly with velocity for velocities up to about 4 km/s. At larger velocities the slope (sensitivity) decreases, becoming zero at about 5 km/s. At still greater velocities the slope is of opposite sign. The number of co-added exposures required to achieve a signal-to-noise ratio of unity is plotted in Fig. A-3. Below about 3 km/s in spacecraft velocity offset, approximately 25 exposures must be co-added to reach SNR=1 for detection of photospheric velocities of 3 m/s, while measurement of photospheric velocities at the level of 1 m/s require that some 250 frames be co-added. In other words, the noise-equivalent velocity-city achieved with 250 co-added frames is about 1 m/s. Above a spacecraft velocity offset of about 4 km/s, the number of frames required to achieve a useful SNR becomes impracticably large.

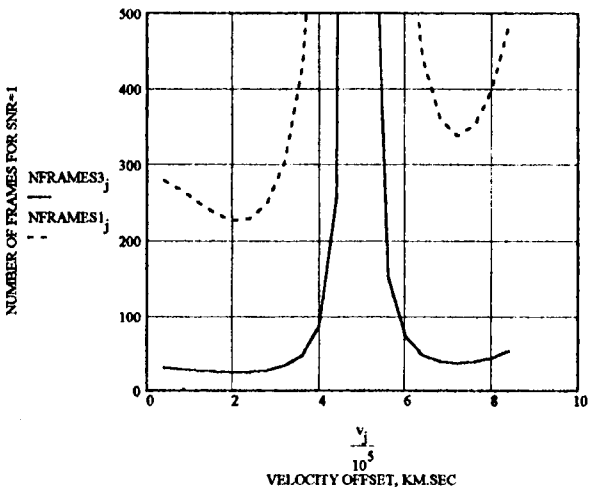

Figure A3. The number of co-added frames, to achieve SNR =1, plotted as function of spacecraft heliocentric speed. The solid and dashed curves represent the noise-equivalent photospheric velocities of 3 m/s and 1 m/s, respectively.

REFERENCES

1. Scherrer, P. H. and the MDI team, "The solar oscillation investigation - Michelson Doppler imager", *Solar Physics*, **162**, 129-188, 1995.
2. Lockhart, R. F., S. H. Pravdo, E. J. Smith, and P. L. Jepsen. "Solar Oscillation Imager Instrument", JPL D-4441 (Internal Document), A Flight Proposal to NASA, Jet Propulsion Laboratory, California Institute of Technology, 1987.
3. Agnelli, G., Cacciani, A., and M. Fofi, The magneto-optical filter, *Solar Physics*, **44**, 509-518, 1975.
4. Cacciani, A., P. Rosati, D. Ricci, A. Egidi, T. Approrchaux, R. J. Marquendant, and E. J. Smith. JPL D-11900 (Internal Document), Jet Propulsion Laboratory, California Institute of Technology, 1994.
5. Cacciani, A., P. F. Moretti, and W. E. Rodgers. "Measuring Doppler and magnetic fields simultaneously", *Solar Physics*, **148**, 1-14, 1997.
6. Mendis, S. K., S. E. Kemeny, R. C. Gee, B. Pain, C. O. Staller, Q. Kim, and E. R. Fossum. "CMOS active pixel image sensors for highly integrated image systems", *IEEE Journal of Solid-State Circuits*, **32**, No. 2, 1997.